EUROPEAN JOURNAL OF BIOMEDICAL AND PHARMACEUTICAL SCIENCES
http://www.ejbps.com

ISSN 2349-8870
Volume: 9
Issue: 8
499-514
Year: 2022

MOLECULAR DOCKING AND MOLECULAR DYNAMICS SIMULATION TO INVESTIGATE PROTEIN-LIGAND BINDING OF POTENTIAL DRUG CANDIDATES FROM VERNONIA AMYGDALINA AGAINST WILMS' TUMOR 1 (WT1) PROTEIN

Leonard O. Ehigie[1], Fiyinfoluwa Demilade Ojeniyi[1], Adesina Rashidat[2], Christopher Igbeneghu[2], Nassar Sulaimon[2] and Adeola Folasade Ehigie[1]*

[1]Department of Biochemistry, Ladoke Akintola University of Technology, Ogbomoso, Nigeria.
[2]Medical Laboraory Science Department, College of Health Sciences, Ladoke Akintola University of Technology, Ogbomoso, Nigeria.

***Corresponding Author: Adeola Folasade Ehigie**
Department of Biochemistry, Ladoke Akintola University of Technology, Ogbomoso, Nigeria.

Article Received on 22/06/2022 **Article Revised on 12/07/2022** **Article Accepted on 01/08/2022**

ABSTRACT
Overexpression of Wilms' Tumor 1 protein **(**WT1) is present in a variety of malignant tumors with a putative role of an oncogene. It plays an important role in the proliferation and inhibition of differentiation of neoplastic cells, making it a suitable therapeutic target, especially for tumor-directed immunotherapy. Vernonia aygdalina (VA) contains different bioactive components such as alkaloids, flavonoids, tannins, saponins, triterpenoids, and many more which are responsible for their its pharmacological properties such as antimalaria, antimicrobial, antioxidant, anti-inflammatory, antidiabetic, antithrombotic, laxative, anticancer, antihelmintic, and hypoglycemic among others. In this investigation, we docked bioactive molecules of VA onto the active site of WT1. Based on their docking scores, 2-methyl azetidine had highest binding energy of -7.2 Kcal moL^{-1}. The conformational behavior of the docked complex was further analyzed via molecular dynamics simulations. The inhibitory potential of these molecules could further be examined by in-vivo and in-vitro investigations to validate its use as an inhibitor against WT1.

KEYWORDS: laxative, anticancer, antihelmintic, and hypoglycemic.

1. INTRODUCTION
Wilms' tumor gene 1 (WT1) has been evaluated as a novel potential prognostic factor, minimal residual disease (MRD) marker and therapeutic target in acute leukemia. The Wilms tumor 1 gene, WT1, encodes a transcription factor involved in normal and malignant hematopoiesis. WT1 was first recognized as a tumor suppressor when congenital malformation syndromes with predisposition to childhood kidney cancer were linked to WT1 germline mutations (Little and Wells, 1997). WT1 is located on chromosome 11p13 and encodes a zinc-finger transcription factor. Post-transcriptional mRNA modifications and the presence of possible several transcription initiation sites give rise to a number of different WT1 protein isoforms (at least 32) that are localized in specific subcellular and subnuclear regions and show different, partially overlapping but distinct functions (Scharnhorstet al., 2001;Sugiyama 2001; Sugiyama 2002).WT1 regulates the transcription of a variety of target genes and is involved in post-transcriptional mRNA processing.

Bitter leaf scientifically known as Vernonia amygdalina is one of the most famous plants found in Africa and Asia. It is the most cultivated species of the genus Vernonia that is about 1,000 species of shrub (Njan et al., 2008; Egharevba et al., 2014). V. amygdalina has been the most prominent species in the family of Asteraceae that had been studied in Africa (Ankit et al., 2010). Normally, V. amygdalina does not produce seeds but its cultivation is usually done by stem planting and mostly grow in tropical areas. This plant is found majorly along the drainage, commercial plantation or forest (Yeap et al., 2010). Several studies had been done in isolating and characterizing some bioactive compounds from V. amygdalina. The phytochemical studies had resulted in the isolation of flavonoids, saponins, alkaloids, tannins, phenolics, terpenes, steroidal glycosides, triterpenoids, and several types of sesquiterpene lactones (Erasto et al., 2006; Kiplimo et al., 2011; Luo et al., 2017). Sesquiterpene lactones (vernodalinol, vernolepin, vernomygdin, hydroxyvernolide, vernolide and vernodalol) had been reported to inhibit breast cancer cell growth, possessed antitumoral and antimicrobial properties, and exhibited a significant bactericidal

activity against gram bacteria (Erasto et al., 2006; Amodu et al., 2013; Luo et al., 2017). This paper aims to study the effect of bioactive compounds in V. amygdalina (Bitter leaf) on Wilms tumor 1 as possible therapeutic candidates in the treatment of diseases associated with the overexpression of WT1.

2. MATERIALS AND METHODS

2.1.1. Datasets

The three dimensional crystal structure of WT1 (PDB ID: 2PRT) having a resolution of 3.15 Å was retrieved from the Protein Data Bank for this study (Stoll et al., 2007). The bioactive molecules of Vernonia amygdalina used as ligand molecules were obtained from pubchem in sdf file format. PubChem database was (pubchem.ncbi.nlm.nih.gov) is a database which provides us with structures of small organic molecules. It also contains information related to its origin and related literatures. It is updated by NCBI. Compounds were downloaded in. sdf file format or chemical (CID) format. Their conformational energy were minimized by using MMFF94 force field.

Drug likeness analysis of A. muricata bioactive compounds

3D structures of the compounds were analyzed using SwissADME, a free online tool to assess small compounds' pharmacokinetics, drug-likeness, and medicinal chemistry friendliness. In the development of therapeutic candidates, physicochemical qualities must be determined at all phases, from research design to pre-clinical trials.

Ligands	2D structure	Pubchem CID	Molecular weight
1,1 dimethyl ethyl ester	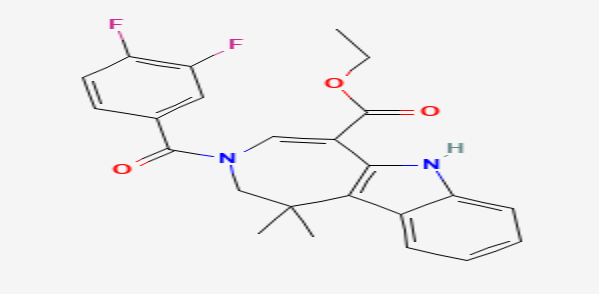	10025364	424.4g/mol
1,3 butanediol	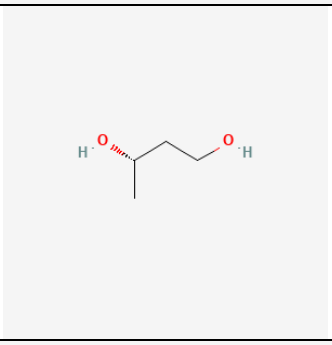	7896	90.12g/mol
1,9-nonanediol	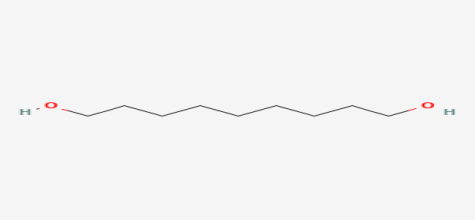	19835	160.25g/mol
1-methyl-5-nitro-4-pyrazolecarboxylic acid	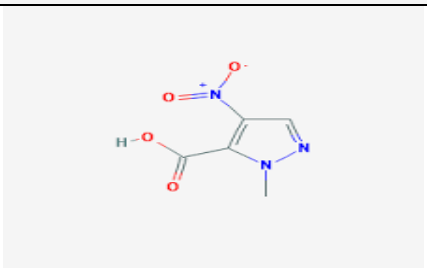	270609	171.11g/mol

1-Tridecyne	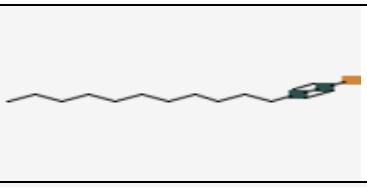	117754	180.33g/mol
2 oxoacetic acid	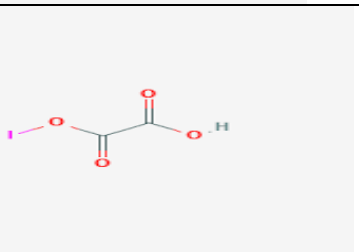	12247702	76.028g/mol
2,3 hexanedione	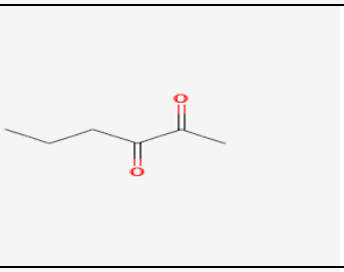	19707	114.14g/mol
2,3 pentanedione	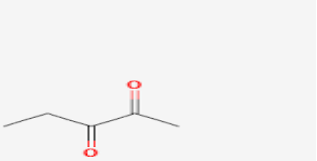	11747	100.12g/mol
2,4 dimethyl-3-pentanol	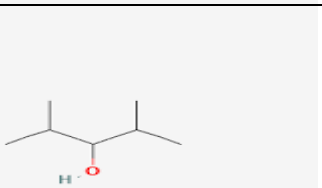	11752	116.2g/mol
2-methyl azetidine	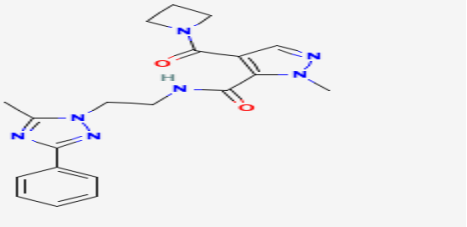	131732422	410.4g/mol
2-Methyl-3-hexanol	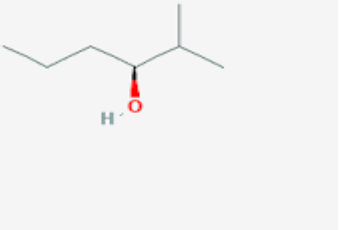	12040	116.2g/mol

2-pentanol	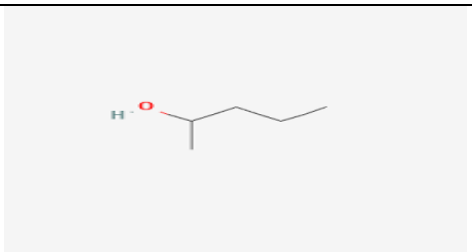	22386	88.15g/mol
2-tridecen-1-ol		5364949	198.34g/mol
8-hexadecyne	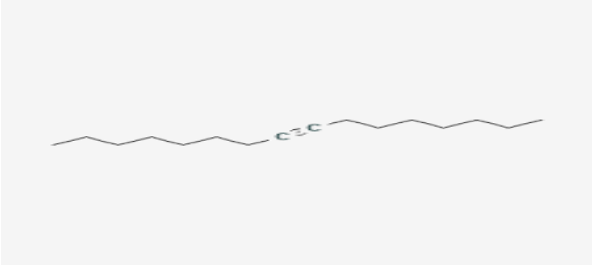	123387	222.41g/mol
9,12,15-octadecatrienoic acid	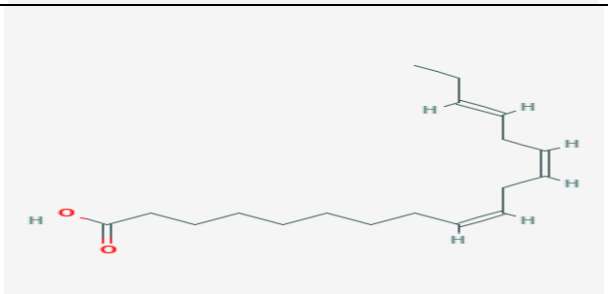	5280934	278.4g/mol
9,12-octadecadienoic acid	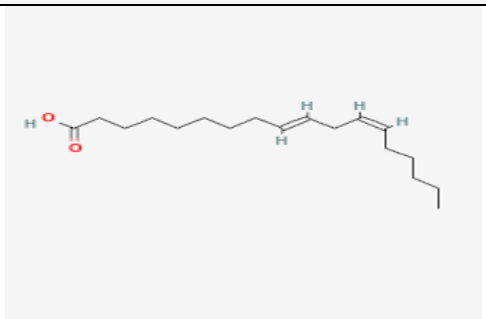	5280450	280.4g/mol
9-octadecenoic acid	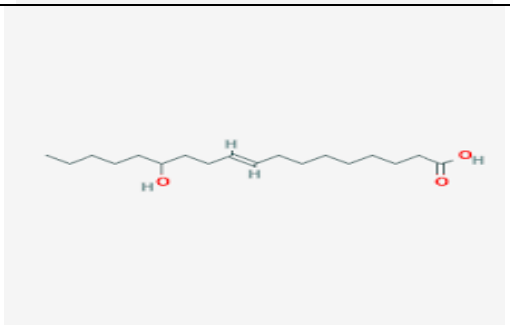	44612156	296.4g/mol

Ascorbic acid	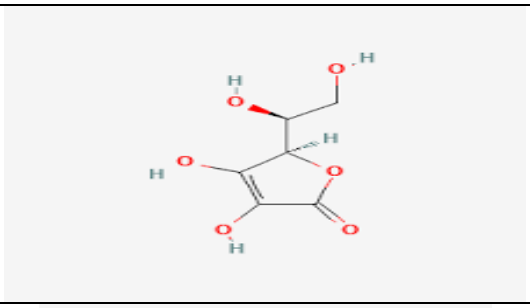	54670067	176.12g/mol
Cysteine	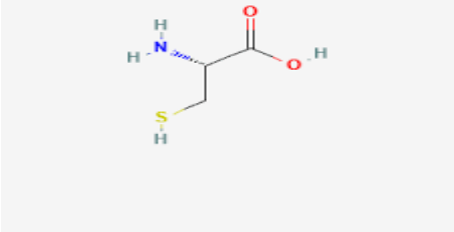	5862	121.16g/mol
Diisooctylphthalate	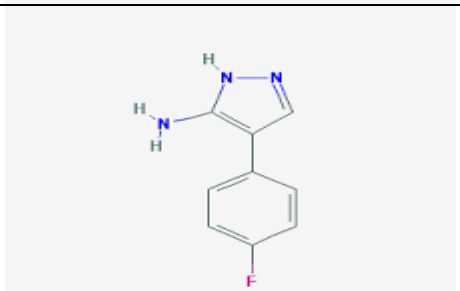	201772	177.18g/mol
Dodecanoic acid	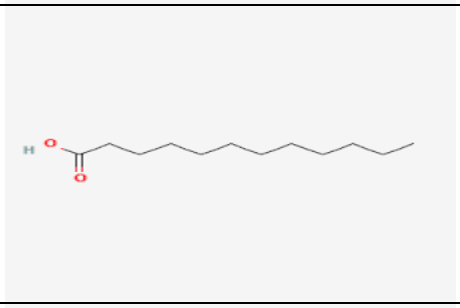	3893	200.32g/mol
Glycine	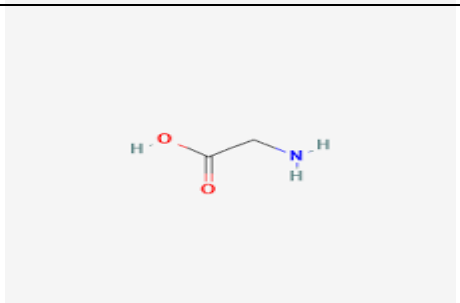	750	75.07g/mol
Hexadecanoic acid	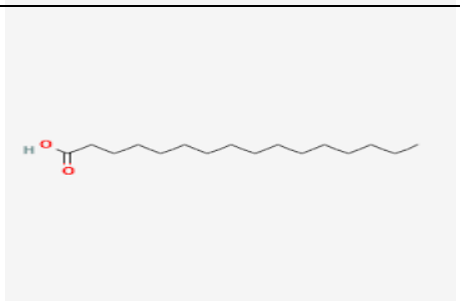	985	256.42g/mol

Hydroxyvernolide	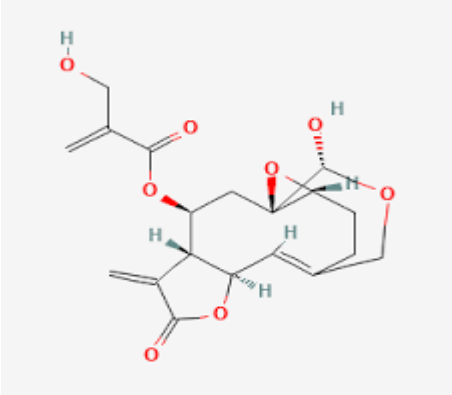	5281472	378.4g/mol
Luteolin	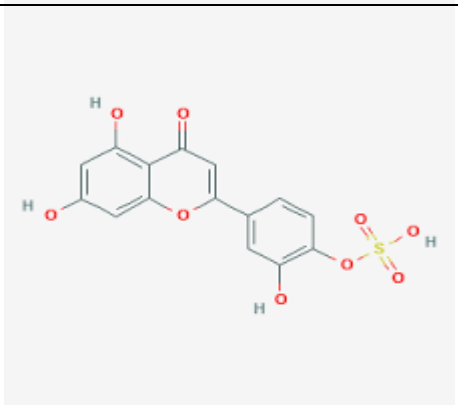	5280445	286.24g/mol
Oxalic acid	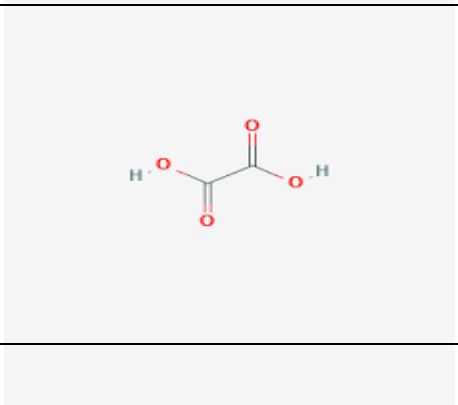	971	90.03g/mol
Oxirane	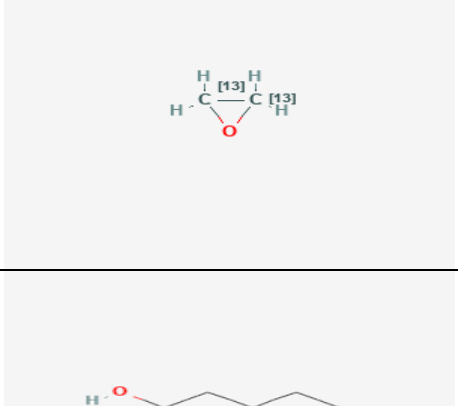	6354	44.05g/mol
Pentanoic acid	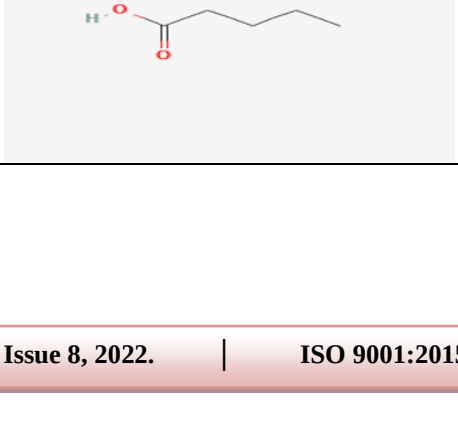	7991	102.13g/mol

Phytol		5280435	296.5g/mol
Pyridoxine	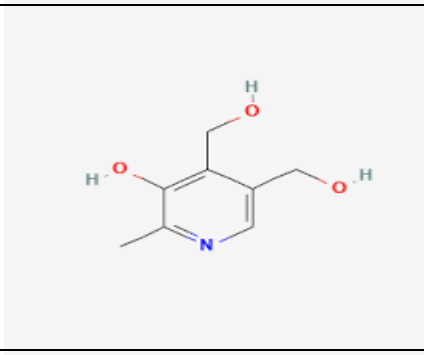	1054	169.18g/mol
Squalene	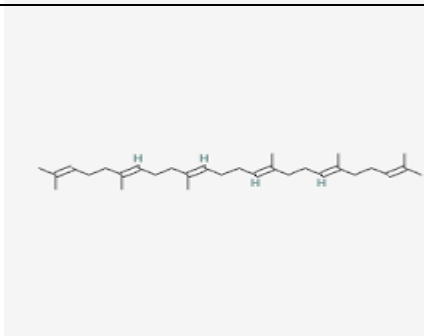	638072	410.7g/mol
Thiamin	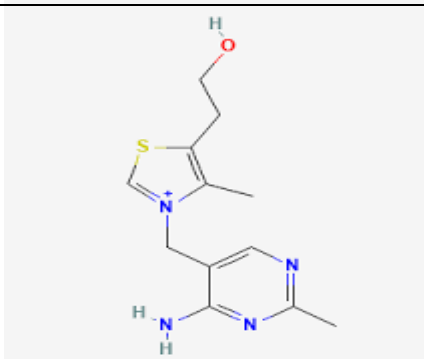	1130	265.36g/mol
Vernodalin	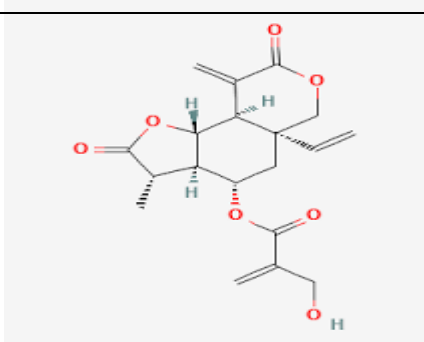	179375	360.4g/mol

Vernodalol	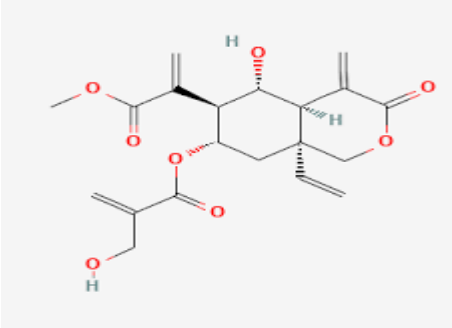	442318	392.4g/mol
Vernolepin	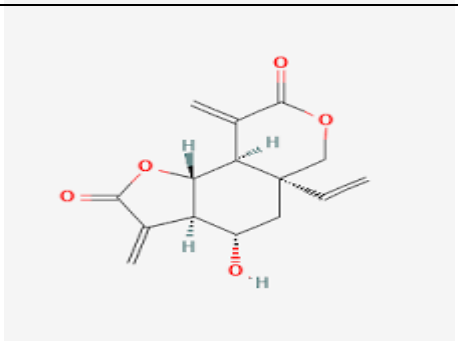	442322	276.28g/mol
Vernolide	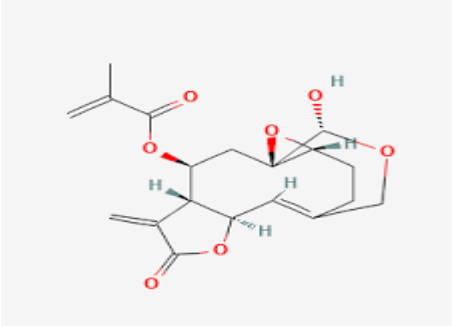	5281508	362.4g/mol
Vernomenin	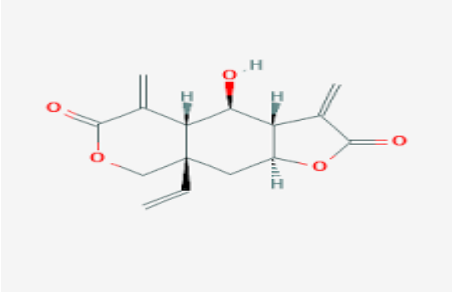	442324	276.28g/mol
Vernomygdin	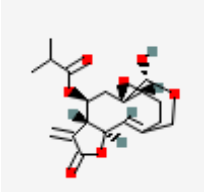	5281509	364.4g/mol
Vitamin E	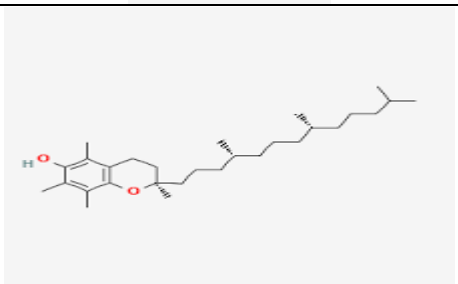	14985	430.7g/mol

Doxorubicin	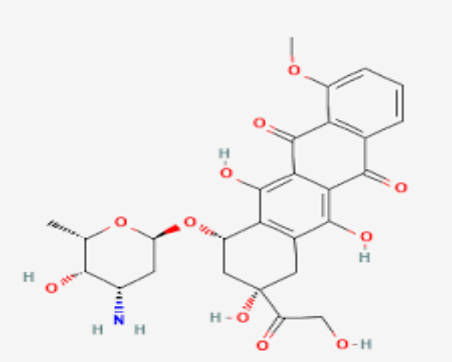	31703	543.5g/mol

Table 2: Drug likeness properties of the tested compounds.

Compounds	Molecular formular	Molecular weight	LogP (<5)	H-bond Donor(<5)	H-bond Acceptor(<10)	Violations	Meet RO5 Criteria
1,1 dimethyl ethyl ester	C23H22F2N2O3	424.44 g/mol	3.49	1	5	0	Yes
1,3 butanediol	C4H10O2	90.12 g/mol	1.26	2	2	0	Yes
1,9-nonanediol	C9H20O2	160.25 g/mol	2.35	2	2	0	Yes
1-methyl-5-nitro-4-pyrazolecarboxylic acid	C5H5N3O4	171.11 g/mol	0.36	1	5	0	Yes
1-Tridecyne	C13H24	180.33 g/mol	3.86	0	0	1	Yes
2 oxoacetic acid	C2H2O3	74.04 g/mol	-0.09	1	3	0	Yes
2,3 hexanedione	C6H10O2	114.14 g/mol	1.74	0	2	0	Yes
2,3 pentanedione	C5H8O2	100.12 g/mol	1.47	0	2	0	Yes
2,4 dimethyl-3-pentanol	C7H16O	116.20 g/mol	2.23	1	1	0	Yes
2-methyl azetidine	C19H22N8O3	410.43 g/mol	2.78	2	7	1	Yes
2-Methyl-3-hexanol	C7H16O	116.20 g/mol	2.32	1	1	0	Yes
2-pentanol	C5H12O	88.15 g/mol	1.88	1	1	0	Yes
2-tridecen-1-ol	C13H26O	198.34 g/mol	3.61	1	1	0	Yes
8-hexadecyne	C16H30	222.41 g/mol	4.62	0	0	1	Yes
9,12,15-octadecatrienoic acid	C18H30O2	278.43 g/mol	3.36	1	2	1	Yes
9,12-octadecadienoic acid	C18H32O2	280.45 g/mol	4.14	1	2	1	Yes
9-octadecenoic acid	C18H32O3	296.44 g/mol	3.62	1	3	0	Yes
Ascorbic acid	C6H8O6	176.12 g/mol	0.39	4	6	0	Yes
Cysteine	C3H7NO2S	121.16 g/mol	o.37	2	3	0	Yes
Diisooctylphthalate	C9H8FN3	177.18 g/mol	1.02	2	2	0	Yes
Dodecanoic acid	C12H24O2	200.32 g/mol	2.70	1	2	0	Yes
Glycine	C2H5NO2	75.07 g/mol	0.37	2	3	0	Yes
Hexadecanoic acid	C16H32O2	256.42 g/mol	3.85	1	2	1	Yes
Hydroxyvernolide	C19H22O8	378.37 g/mol	1.83	2	8	0	Yes
Luteolin	C15H10O6	286.24 g/mol	1.86	4	6	0	Yes
Oxalic Acid	C2H2O4	90.03 g/mol	-0.35	2	4	0	Yes
Oxirane	C2H4O	44.05 g/mol	1..17	0	1	0	Yes
Pentanoic Acid	C5H10O2	102.13 g/mol	1.32	1	2	0	Yes
Phytol	C20H40O	296.53 g/mol	4.71	1	1	1	Yes
Pyridoxine	C8H11NO3	169.18 g/mol	0.80	3	4	0	Yes
Squalene	C30H50	410.72 g/mol	6.37	0	0	1	Yes
Thiamin	C12H17N4OS	265.35 g/mol	-1.60	2	3	0	Yes
Vernodalin	C19H20O7	360.36 g/mol	2.25	1	7	0	Yes
Vernodalol	C20H24O8	392.40 g/mol	3.27	2	8	0	Yes
Vernolepin	C15H16O5	276.28 g/mol	1.71	1	5	0	Yes
Vernolide	C19H22O7	363.37 g/mol	2.48	1	7	0	Yes
Vernomenin	C15H1605	276.28 g/mol	1.77	1	5	0	Yes
Vernomygdin	C19H24O7	364.39 g/mol	2.48	1	7	0	Yes
Vitamin E	C29H50O2	430.71 g/mol	5.92	1	2	1	Yes

Molecular Docking study

The three dimension structure of protein and ligands were prepared in pdb format. Molecular docking simulation was run by PyRx. PyRx is a Virtual Screening software for Computational Drug Discovery that can be used to screen libraries of compounds against potential drug targets. PyRx enables Medicinal Chemists to run Virtual Screening from any platform and helps users in every step of this process - from data preparation to job submission and analysis of the results. While it is true that there is no magic button in the drug discovery process, PyRx includes docking wizard with easy-to-use user interface which makes it a valuable tool for Computer-Aided Drug Design. PyRx also includes chemical spreadsheet-like functionality and powerful visualization engine that are essential for Rational Drug Design. The AutodockTools (ADL) was utilized in minimizing energy and adding the partial charges of polar hydrogens of receptor (protein). The ligands were prepared with flexible torsion angles and the protein was prepared in a static (rigid) form. Furthermore, protein and ligands were kept in pdbqt formats which suitable for docking simulation. The affinity binding were calculated as total intermolecular energies (kcal/mol) which involved hydrogen bond, Van Der Walls force, desolvation and electrostatic energies. On the other hand, the apropriate torsion angles of ligand is also induced as internal ligand energy. The docking program evaluated the lowest binding energy (LBE) to obtain the best binding mode. The Root-Mean-Square Deviation (RMSD) which less than 2.0 Å was scored during running docking program.

Molecular Dynamics Simulations

The GROMACS (Version 2018) was utilized to perform MD simulation (Abraham et al., 2015). GROMOS54a7 force field and single-point charge (SPC) water model was applied to conduct MD simulation of all complexes. Topologies and parameter files of the lead compounds and the standard inhibitor were generated using PRODRG server (Schüttelkopf and Van Aalten, 2004). All the complexes were simulated inside a cubic box with 1 Å of buffer distance. For the electro neutralization of the complexes, the respective number of ions were added. Bad contacts and clashes in the protein were resolved by energy minimization using 5,000 steps of steepest decent method. Following the energy minimization, all the complexes underwent two steps of equilibration, first 100 ps of NVT equilibration followed by 100 ps of NVT equilibration. In order to avoid the cold solute–hot solvent difficulty, temperature coupling was applied, which was achieved by indexing the system into non-water and water components by using gmx make_ndx module of GROMACS (Lemkul, 2019). The temperature of the system was maintained at 300°C by using Berendsen thermostat (Berendsen et al., 1995). Similarly, the pressure of the system was maintained by using Parrinello-Rahman barostat (Parrinello and Rahman, 1981). Long-range interaction present in the system was treated by applying the LINCS method (Hess et al., 1997). MD simulations were performed for 20,000 ps, and the coordinates were saved at every 1 ps for all the system. Structural and conformational analysis of all system was conducted using various analysis modules implemented in GROMACS package.

RESULT

Table 1: Protein–ligand interaction profiles. The table reveals the various interactions and binding affinities.

Ligands	Number of hydrogen bonds	Binding affinity	Interaction/Distance
1,1 dimethyl ethyl ester	2	-7.2	ARG(A:376)-2.91 ARG(A:376)-2.91
1,3 butanediol	3	-3.3	ARG(A:372)-2.29 ARG(A:372)-2.29 GLN(A:369)-1.96
1,9-nonanediol	3	-3.8	ARG(A:372)-2.29 ARG(A:376)-2.91 GLN(A:369)-2.38
1-methyl-5-nitro-4-pyrazolecarboxylic acid	4	-4.9	ARG(A:372)-2.29 ARG(A:372)-2.29 HIS(A:373)-3.07 HIS(A:373)-3.07
1-Tridecyne	None	-4.4	None
2 oxoacetic acid	3	-3.1	ARG(A:372)-2.07 ARG(A:375)-2.05 SER(A:395)-2.26
2,3 hexanedione	4	-3.9	ARG(A:394)-2.19 ARG(A:372)-2.57 ARG(A:372)-2.57 HIS(A:373)-3.03
2,3 pentanedione	4	-3.7	ARG(A:372)-2.39 ARG(A:372)-2.17 ARG(A:394)-2.35

			HIS(A:373)-2.88
2,4 dimethyl-3-pentanol	None	-3.8	None
2-methyl azetidine	2	-7.2	ASP(A:396)-2.50 THR(A:400)-2.50
2-Methyl-3-hexanol	1	-3.7	ARG(A:372)-2.27
2-pentanol	None	-3.1	None
2-tridecen-1-ol	None	-4.0	None
8-hexadecyne	None	-4.4	None
9,12,15-octadecatrienoic acid	2	-4.6	ARG(A:372)-2.81 SER(A:393)-2.68
9,12-octadecadienoic acid	2	-4.7	ARG(A:394)-2.45 HIS(A:397)-2.00
9-octadecenoic acid	2	-4.2	HIS(A:373)-2.66 SER(A:393)-2.78
Ascorbic acid	2	-4.9	ARG(A:372)-2.33 ARG(A:372)-2.10
Cysteine	5	-3.3	GLU(A:350)-2.10 GLU(A:350)-2.85 GLU(A:350)-2.92 SER(A:365)-2.49 SER(A:365)-2.83
Diisooctylphthalate	2	-5.1	ARG(A:372)-2.51 ARG(A:372)-2.60
Dodecanoic acid	2	-4.5	HIS(A:373)-4.99 SER(A:393)-2.90
Glycine	4	-3.2	GLU(A:350)-2.92 HIS(A:347)-2.18 SER(A:365)-2.29 SER(A:365)-2.53
Hexadecanoic acid	None	-4.3	None
Hydroxyvernolide	5	-6.5	ARG(A:372)-2.13 ARG(A:372)-2.08 ARG(A:394)-2.65 HIS(A:373)-2.68 SER(A:393)-2.39
Luteolin	2	-7.1	ARG(A:376)-2.54 GLN(A:369)-2.51
Oxalic acid	4	-3.4	ARG(A:372)-3.06 ARG(A:375)-1.97 ARG(A:375)-2.03 SER(A:393)-2.30
Oxirane	1	-1.9	SER(A:395)-1.86
Pentanoic acid	1	-3.6	ARG(A:394)-2.27
Phytol	1	-5.2	SER(A:393)-2.11
Pyridoxine	3	-4.6	ARG(A:394)-2.40 ARG(A:362)-2.40 GLN(A:369)-2.78
Squalene	None	-5.7	None
Thiamin	3	-4.9	ARG(A:372)-2.23 ARG(A:372)-2.88 GLN(A:369)-2.55
Vernodalin	4	-6.6	ARG(A:372)-2.86 ARG(A:372)-2.00 ARG(A:394)-2.34 GLN(A:369)-2.07
Vernodalol	6	-5.4	ARG(A:372)-2.81 ARG(A:372)-2.42 ARG(A:372)-2.60 ARG(A:394)-2.25

			ARG(A:394)-2.22 ARG(A:376)-2.06
Vernolepin	3	-6.3	ARG(A:362)-2.39 ARG(A:372)-2.16 ARG(A:394)-2.35
Vernolide	2	-6.2	THR(A:400)-2.41 THR(A:400)-2.83
Vernomenin	1	-6.2	ARG(A:372)-2.13
Vernomygdin	1	-6.1	ARG(A:362)-2.27
Vitamin E	1	-6.1	ARG(A:424)-2.68
Doxorubicin	4	-6.9	ARG(A:362)-2.99 ARG(A:372)-2.04 ARG(A:372)-2.53 ARG(A:376)-2.20

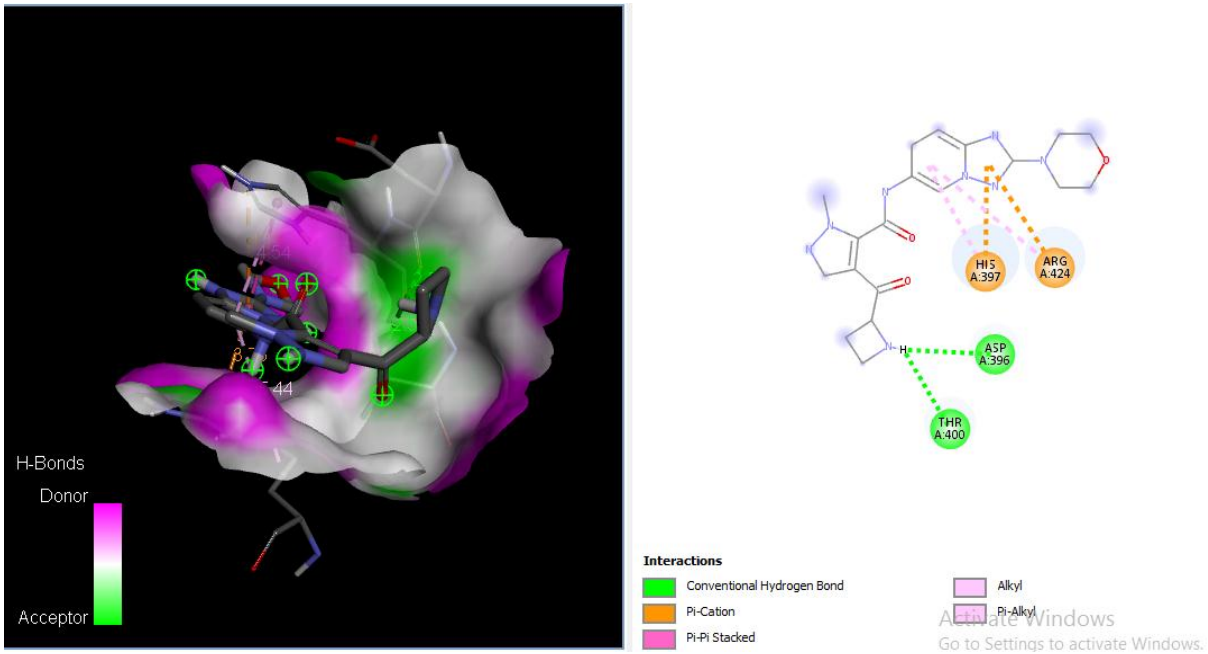

Fig.6: 2D and 3D representation of 2 Methyl azetidine in complex with Wilms Tumor 1 (WT1)

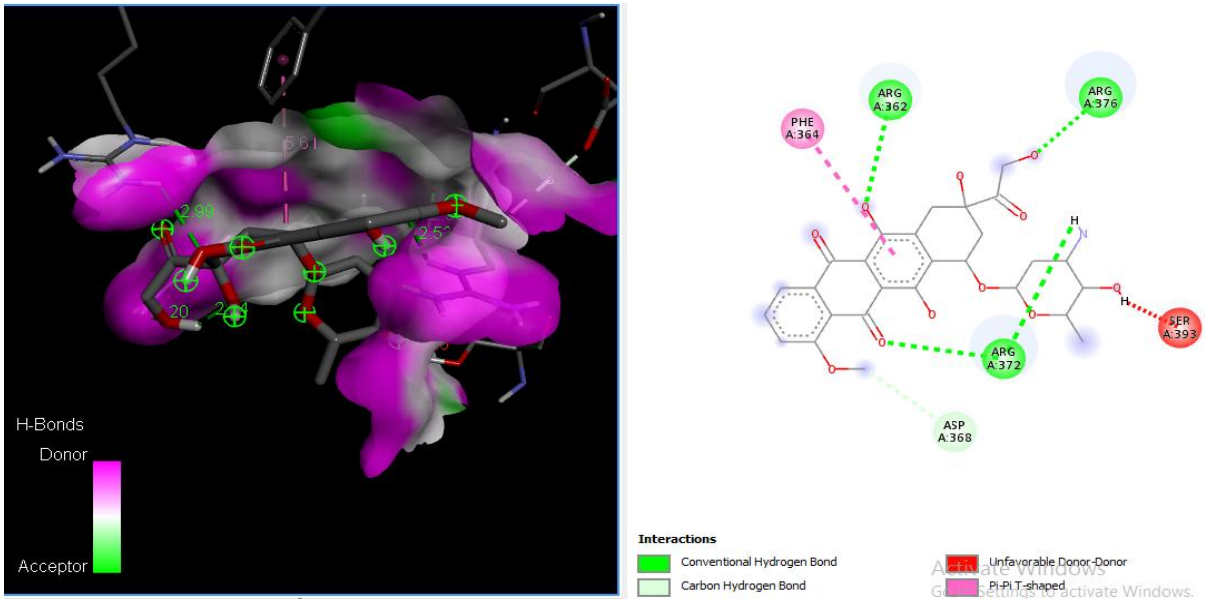

Fig.7: 2D and 3D representation of Doxorubicin(standard drug) with Wilms Tumor 1 (WT1)

Stability and Residue Mobility Analyses
Molecular Dynamics (simulation) trajectory

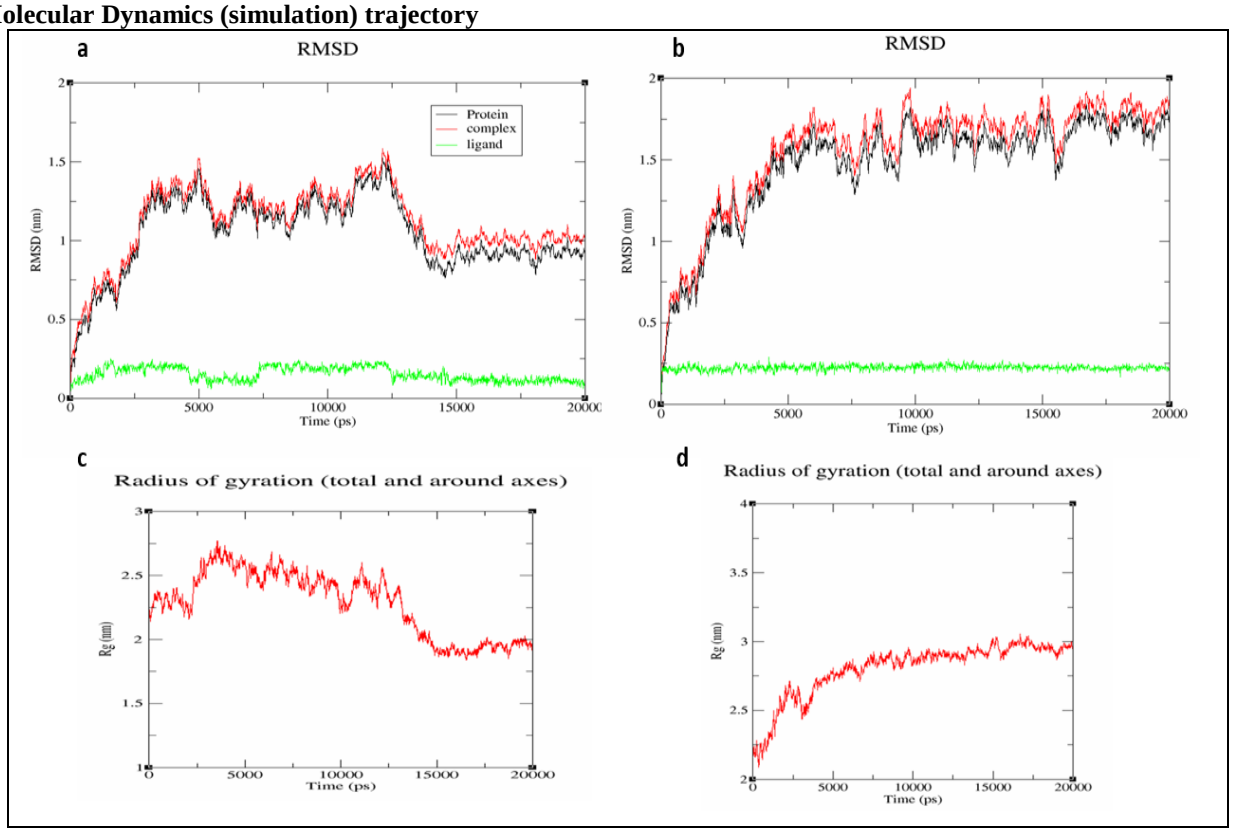

Figure 8: Conformational stability of the WT1 complex with (a) 2-Methyl azetidine complex. (b) doxorubicin. Green line - complex system. Black line - apo structure. Red line - ligand only. (c) Radius of gyration of WT1-2-Methyl azetidine (d) Radius of gyration of WT1-doxorubicin.

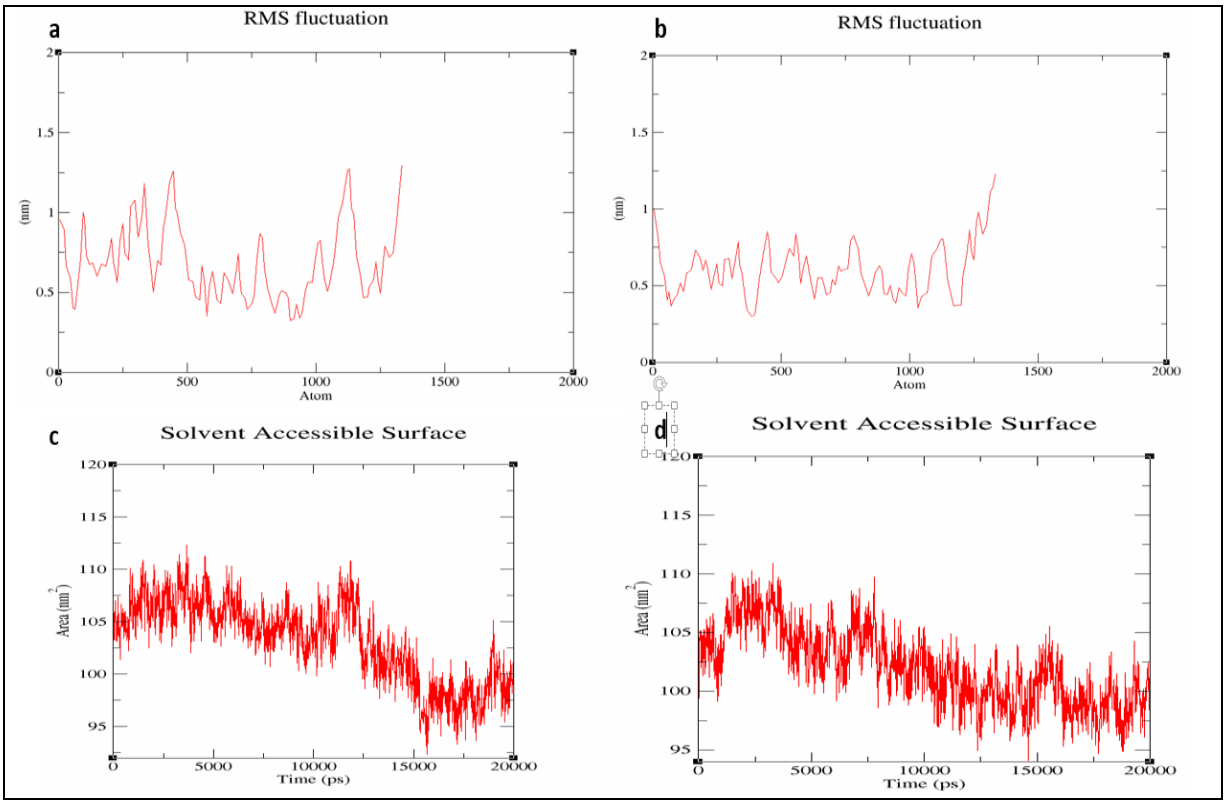

Figure 9: Residue fluctuation (a) and (b) and solvent accessible surface (c) and (d) of the complex systems.

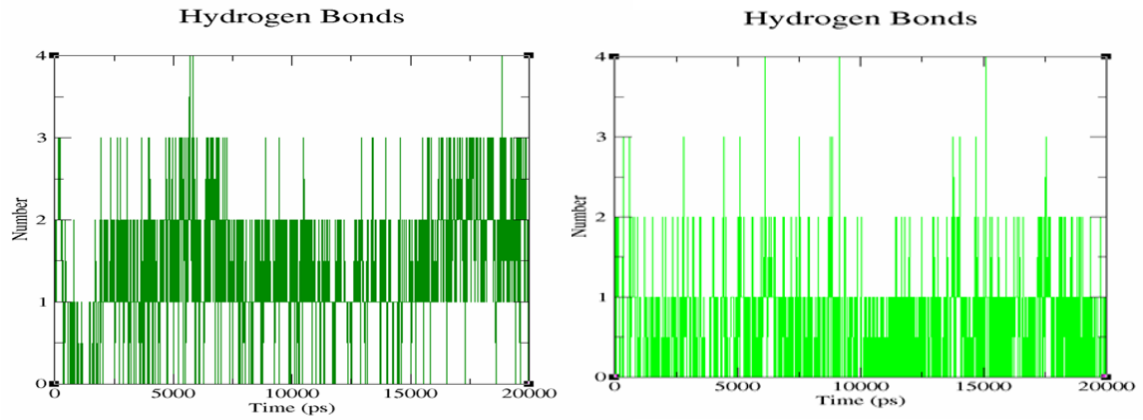

Figure 10: The average number of intermolecular H-bonds of (a) WT1-2-Methyl-azetidine complex and (b) WT1-doxorubicin during a 20 ns MD simulation.

DISCUSSION AND CONCLUSION

DISCUSSION

As observed in the result above, Conventional hydrogen bond play a significant role in the determination of protein affinity for each ligand, also the lower the conformational energy, the higher the affinity for specific protein (Seo et al., 2014), each of the ligands contains an internal nucleus with a positive electric charge, the nucleus is surrounded by electrons with a negative charge (Makedonas and Mitsopoulou, 2006). WT1 was docked with thirty nine (39) ligands. The analysis of the docked proteins with the ligands revealed favorable docking pose Out of the 39 Ligands for the protein shown in Table 3,ligand with highest hydrogen bond and high binding affinity was chosen as the best ligandfor the protein.Fig 10 shows the interaction of the best ligand 2 methyl azetidine with Wilms Tumor 1 (PDB CID; WT1)receptor forming 2 hydrogen bond interaction at amino acid position ASP396 and THR400 with binding affinity of -7.2.Fig 7 indicate doxorubicin (standard drug) which has 4 hydrogen bond interaction at amino acid position ARG362, ARG372, ARG372, and ARG376 with -6.9 binding affinity for WT1.

As said earlier, the hydrogen bond level plays a significant role in the determination of protein affinity to each ligand. Each of the ligand contains an internal nucleus with positive and negative electric charges.The nucleus is surrounded by electron with a negative charge (Makedonas and Mitsopoulou, 2006). Fig 6 shows the hydrogen binding of the amino acids present in the protein to the peptide. The figure further reveals the pointof binding in the active (interacting residue) residue as C-H (conventional hydrogen main chain), CH (carbon hydrogen side chain).Alky, and Pi-alkyl group.

The ligand with the optimal binding potency and selectivity, as well as favourable intestinal absorption, requires a balance of lipophilic and hydrogen bonding groups. Lipinski's rules of five (Ro5) was instrument in giving medicinal chemist towards an improved balance of properties within a drug molecule (Alex et al., 2011). Ro5 suggest poor oral absorption is more likely when molecular weight (Mw) is >500 Da, the hydrogen bond (H-bond) acceptor count (N/O count) is >10, the H-bond donor count (NH/OH) is >5, and the clogP is >5.4. The hypothesis follows that not failing more than one of these guide line should lead to a reduced pharmaco-kinetics related attribution in early development.

2 methyl azetidine compound interact with the WT1 a mutated protein in ALL and helps to inhibit its activity. It interacts with so many means as showing the binding affinity through the hydrogen bonding as shown in the result above. 2 methyl azetidine is confirming to be very important as an antineoplastic agent and also the binding interaction of the hydrogen bond between the complex is explained above. All the above studied compounds were potential antineoplastic agents on WT1. Molecular docking of a target protein involves finding the best orientation or conformation of a protein at possible binding site of the receptor, evaluating its energy/bonding score and ranked according to their scores or values (Brooijmans and Kuntz, 2003; Halperin et al., 2002).

The mechanisms by which protein receptor recognizes its ligand and interact with those molecular substrates are much importance in docking. Binding and interaction of protein and ligand enable the prediction and ranking of substrate (Sousa et al., 2006).

From the docking analysis, the ligand 2 methyl azetidine was selected to perform molecular dynamics simulation study, because it was the one that shows the highest binding interaction and conformational hydrogen bound, the simulation was carried out on system to study the dynamics behaviour of the targeted protein.

The molecular dynamic simulation trajectory reveals the stability of the protein-ligand configurations in prior to and after simulation and can be measured using the following indices: Radius of gyration, root mean square deviation, root mean square fluctuation, solvent accessible surface area, and hydrogen bond interaction.

Radius of gyration indicate that at 2.5nm, the atom exhibit a strong stability and shows that a compactness occurs until 2nm at time interval of 2500 to 100000ps, as the graph proceed, the atoms loses its compactness and become less stable at time interval of 10000ps to 15000ps. Lastly from 15000ps to the end of simulation, the atom regain back its stability and said to be more compact compared to the sarting point. The difference is partly caused by limitations in the forcefield, but also because atoms in the simulation are moving and vibrating around an equilibrium structure. A better measure can be obtained by first creating a running average structure from the simulation and comparing the running average with the x-ray structure, which gives a more realistic Gyrate around 2.9nm.

The RMSD plot illustrated in Figure 8 Shows that the RMSD of the complex fluctuate at 0.05(nm) with a slight fluctuation near 1.5 (nm) and the fluctuation peaks lower near the end of the simulation. This shows that the structure is less stable, because the lower the RMSD the lower the structural deviation and the higher the stability.

Root Mean Square Fluctuations that are greater than 0.25 nm are of interest. For example, the fluctuation near atom position 500, the atom at 500, the one near 1250, 1500, the atom at 2500 and the one near 2750. They are the major atoms that constitute to the overall structure of protein in the RMSD; also there is really not much fluctuation since it occurs between 0.25 to 0.5. To consider the particular atoms in the complex, (i.e. the particular atom out of the complex that partakes in the fluctuation) they are inspected with molecular visualization software such as VMD. The difference is partly caused by limitations in the forcefield, but also because atoms in the simulation are moving and vibrating around an equilibrium structure. A better measure can be obtained by first creating arunning average structure from the simulation and comparing the running average with the x-ray structure, which gives a more realistic RMSF around 1500 atom.

The SASA is also illustrated in Figure 10. The plot shows that the atom shows a rigid compactness and they are more stable around the surface area solvent. It decreases below 105nm^2 but stabilizes at 110nm^2 and then decreases till the end of the simulation. The difference is partly caused by limitations in the forcefield, but also because atoms in the simulation are moving and vibrating around an equilibrium structure.

CONCLUSION

Wilms Tumor 1(WT1) a mutated protein in ALL plays an important role in the manifestation of the disease. Organic compounds in Vernonia amygygdalina (Bitter leaf) which are known to have antineoplastic properties were used for docking with the target WT1 (protein). The analysis of the docked complexes revealed the molecular interaction between them. The binding pattern of the amino acid residues participate in the interaction energies of the docked complexes. Applying Linpinski's rule, thirty nine bioactive compounds of bitter leaf were validated as valid drugs and docked with WT1 which shows good negative binding energy values. A more negative binding energy value could form stable complex with the receptor and it was seen in the interaction of 2 methyl azetidine which was -7.2 Kcal moL^{-1}. The lesser binding energy value inferred that the compound had higher affinity toward the receptor and the binding was in a stable conformation confirmed via dynamics simulation and thus may have anti-neoplastic potential.

REFERENCES

1. Amodu, A., Itodo, S. E., and Musa, D. E. (2013). Nigerian Foodstuffs with TumourChemosuppressive Polyphenols. International Journal of Pharmaceutical Science Invention, 2(1): 12–17.
2. Ankit Saneja, Chetan Sharma, K.R., and Aneja, R. P. (2010). Bitterleaf as Local Substitute for Hops in the Nigerian Brewing Industry. Pharmaci, 2(2): 208–220.
3. Berendsen, H. J., van der Spoel, D., & van Drunen, R. (1995). GROMACS: A message-passing parallel molecular dynamics implementation. Computer physics communications, 91(1-3): 43-56.
4. Brooijmans, N., and Kuntz, I. D. (2003).Molecular recognition and docking algorithms.Annual review of biophysics and biomolecular structure, 32(1): 335-373.
5. Danchin, A., Médigue, C., Gascuel, O., Soldano, H., and Hénaut, A. (1991) From data banks to data bases.Research in Microbiology, **142**(7–8): 913–916.
6. Egharevba, C., Osayemwenre, E., Imieje, V., Ahomafor, J., Akunyuli, C., Udu-Cosi, A. A., Theophilus, O., James, O., Ali, I. and Falodun, A. (2014). Significance of Bitter Leaf (Vernonia amgdalina) In Tropical Diseases and Beyond.A Review. Malaria Chemotherapy Control and Elimination, 3(1): 1–10.
7. Erasto, P., Grierson, D. S., and Afolayan, A. J. (2006). Bioactive Sesquiterpene Lactones from the Leaves of Vernonia amygdalina. Journal of Ethnopharmacology, 106: 117–120.
8. Halperin, I., Ma, B., Wolfson, H., and Nussinov, R. (2002). Principles of docking: An overview of search algorithms and a guide to scoring functions. Proteins: Structure, Function, and Bioinformatics, 47(4): 409-443.
9. Hess, B., Kutzner, C., van der Spoel, D., & Lindahl, E. (2008). GROMACS 4: Algorithms for highly efficient, load-balanced, and scalable molecular simulation. Journal of Chemical Theory and Computation, 4(3): 435–447. https://doi.org/10.1021/ct700301q.
10. Kiplimo, J.J., Koorbanally, N.A., and Chenia, H. (2011). Triterpenoids from Vernonia auriculifera Hiern exhibit antimicrobial activity. African Journal of Pharmacy and Pharmacology, 5: 1150–1156.

11. Lee, Vannajan Sanghiran; Chong, Wei Lim; Sukumaran, Sri Devi; Nimmanpipug, Pivarat; Letchumanan, Vengadesh; Goh, Bey Hing; Lee, Learn-Han; Md. Zain, Sharifuddin; Abd Rahman, Noorsaadah (2020).Computational screening and identifying binding interaction of anti-viral and anti-malarial drugs: Toward the potential cure for SARS-CoV-2. Progress in Drug Discovery & Biomedical Science, **3**.
12. Lemkul, J. A. (2019). Gromacs tutorial: Lysozyme in water.
13. Little, M., and Wells, C. (1997). A clinical overview of WT1 gene mutations. Hum Mutat, 9(3): 209–25.
14. Luo, X., Jiang, Y., Fronczek, F. R., Lin, C., Izevbigie, E. B., Lee, S., and Lee, K. S. (2017). Isolation and Structure Determination of a Sesquiterpene Lactone (Vernodalinol) from Vernonia amygdalina Extracts. Pharmaceutical Biology, 49(5): 464–470
15. Makedonas, C., and Mitsopoulou, C. A. (2006). The Relationship BetweenAromaticity and Charge- Transfer Transitions: A Combined Study of Square- Planar Metal.
16. Marino, B.S., and Fine, K.S. (2013). Blueprints Pediatrics. Lippincott Williams & Wilkins. p 205.
17. National Cancer Institute. (2017). Childhood Acute Lymphoblastic Leukemia Treatment. Retrieved 20 December 2017.
18. Njan, A. A., Adzu, B., Agaba, A. G., Byarugaba, D., Díaz-Llera, S., and Bangsberg, D. R. (2008). The Analgesic and Antiplasmodial Activities and Toxicology of Vernonia amygdalina. Journal of Medicinal Food, 11(3): 574–581.
19. Parrinello M, Rahman A (1981) Polymorphic transitions in single crystals: a new molecular dynamics method. J Appl Phys, 52: 7182–7190.
20. Scharnhorst, V., van der Eb, A.J., and Jochemsen, A.G. (2001). WT1 proteins: functions in growth and differentiation. Gene, **273**: 141–161.
21. Schüttelkopf, A. W., & Van Aalten, D. M. (2004). PRODRG: a tool for high-throughput crystallography of protein–ligand complexes. Acta Crystallographica Section D: Biological Crystallography, 60(8): 1355-1363.
22. Seo, M. H., Park, J., Kim, E., Hohng, S., and Kim, H. S. (2014). Protein conformational dynamics dictate the binding affinity for a ligand. Nature communications, 5(1): 1-7.
23. Sousa, S. F., Fernandes, P. A., and Ramos, M. J. (2006). Protein–ligand docking: current status and future challenges. Proteins: Structure, Function, and Bioinformatics, 65(1): 15-26.
24. Stoll, R., Lee, B. M., Debler, E. W., Laity, J. H., Wilson, I. A., Dyson, H. J., & Wright, P. E. (2007). Structure of the Wilms tumor suppressor protein zinc finger domain bound to DNA. Journal of molecular biology, 372(5): 1227–1245. https://doi.org/10.1016/j.jmb.2007.07.017.
25. Sugiyama, H. (2001). Wilms' tumor gene WT1: its oncogenic function and clinical application. Int J Hematol, **73**: 177–187.
26. Sugiyama, H. (2002). Wilms tumor gene WT1 as a tumor marker for leukemic blast cells and its role in leukemogenesis. Methods Mol Med, **68**: 223–237.
27. Yeap, S. K., Ho, W. Y., Beh, B. K., Liang, W. S., Ky, H., Hadi, A., and Alitheen, N. B. (2010). Vernonia amygdalina, an Ethnomedical used Green Vegetable with Multiple Bio-activities. Journal of Medicinal Plants Research, 4(25): 2787–2812.